Energy Conversion and Management 253 (2022) 115187

Contents lists available at ScienceDirect

Energy Conversion and Management

journal homepage: www.elsevier.com/locate/enconman

Techno-Economic assessment of natural gas pyrolysis in molten salts

Florian Pruvost [a], Schalk Cloete [b], Jan Hendrik Cloete [b], Chaitanya Dhoke [b], Abdelghafour Zaabout [b,*]

[a] Génie Chimique, Toulouse INP-ENSIACET, Toulouse, France
[b] Process Technology Department, SINTEF Industry, Trondheim, Norway

ARTICLE INFO

Keywords:
Molten salt pyrolysis
Natural gas pyrolysis
Hydrogen, techno-economic assessment

ABSTRACT

Steam methane reforming with CO_2 capture (blue hydrogen) and water electrolysis based on renewable electricity (green hydrogen) are commonly assumed to be the main supply options in a future hydrogen economy. However, another promising method is emerging in the form of natural gas pyrolysis (turquoise hydrogen) with pure carbon as a valuable by-product. To better understand the potential of turquoise hydrogen, this study presents a techno-economic assessment of a molten salt pyrolysis process. Results show that moderate reactor pressures around 12 bar are optimal, and that reactor size must be limited by accepting reactor performance well below the thermodynamic equilibrium. Despite this challenge stemming from slow reaction rates, the simplicity of the molten salt pyrolysis process delivers high efficiencies and promising economics. In the long-term, carbon could be produced for 200–300 €/ton, granting access to high-volume markets in the metallurgical and chemical process industries. Such a scenario makes turquoise hydrogen a promising alternative to blue hydrogen in regions with public resistance to CO_2 transport and storage. In the medium-term, expensive first-of-a-kind plants could produce carbon around 400 €/ton if hydrogen prices are set by conventional blue hydrogen production. Pure carbon at this cost level can access smaller high-value markets such as carbon anodes and graphite, ensuring profitable operation even for first movers. In conclusion, the economic potential of molten salt pyrolysis is high and further demonstration and scale-up efforts are strongly recommended.

1. Introduction

The established idea of a hydrogen economy is currently enjoying a surge of attention due to rising climate ambitions worldwide. A dedicated hydrogen report from the International Energy Agency [1] investigates all aspects of the hydrogen economy, listing blue (fossil fuels with CCS) and green (water electrolysis using renewable electricity) as the main supply options.

However, there is another promising alternative in the form of natural gas pyrolysis where the fuel is cracked to hydrogen and carbon in a liquid bath of molten metal or salt. Known as turquoise hydrogen, this process enjoys significant advantages relative to blue hydrogen. Given that it requires no process steam or CO_2 capture and compression, it may deliver higher conversion efficiencies. The high efficiency and simple plant layout also promise improved economics. Furthermore, natural gas pyrolysis avoids the political challenges hampering the establishment of CO_2 transport and storage infrastructure in various world regions by producing a valuable pure carbon product instead of a CO_2 waste stream.

From an economic perspective, the cost at which the carbon product can be sold determines the potential of the natural gas pyrolysis process [2]. High-value markets exist for pure carbon, but these markets are orders of magnitude smaller than the expected future market for hydrogen. Thus, if turquoise hydrogen is limited only to these markets, it will remain a minor player in the hydrogen economy. However, if carbon production costs can be brought down to the levels required to compete with high-grade coal in metallurgical and chemical industries, the technical potential of turquoise hydrogen expands greatly. Pure carbon from pyrolysis will enjoy a substantial advantage over coal in these applications as it has higher energy density and does not produce ash or other harmful pollutants.

In recent decades, research on methane pyrolysis has witnessed substantial growth focussing on eliminating the technical barriers hindering the process feasibility, scale up and industrial deployment [3]. Despite thermodynamic equilibrium predicting high conversion rates at temperatures similar to SMR process (800–900 °C) [4], research studies reported temperatures exceeding 1200 °C for achieving acceptable

* Corresponding author at: Flow Technology Group, SINTEF Industry, S.P. Andersens vei 15 B, 7031 Trondheim, Norway.
E-mail address: abdelghafour.zaabout@sintef.no (A. Zaabout).

https://doi.org/10.1016/j.enconman.2021.115187
Received 17 November 2021; Received in revised form 25 December 2021; Accepted 28 December 2021
Available online 5 January 2022

Nomenclature

Acronyms:

ACF	Annualized cash flow
CCS	Carbon capture and storage
LCOC	Levelized cost of carbon
NPV	Net present value
PSA	Pressure swing adsorption
SMR	Steam methane reforming

Main symbols:

C	Molar concentration (mol/m^3)
E_A	Activation energy (kJ/mol)
g	Gravitational acceleration (9.81 m/s^2)
H	Liquid bath height (m)
k	Reaction rate constant (1/s)
k_0	Reaction rate constant pre-exponential factor (1/s)
R	Universal gas constant (8.314 J/(mol.K))
T	Temperature (K)
U	Velocity or superficial velocity (m/s)
ϵ	Volume fraction
μ	Dynamic viscosity (kg/(m.s))
ρ	Density (kg/m^3)
σ	Surface tension (N/m)

Sub- and superscripts:

eq	Equilibrium value
in	Inlet value
G	Gas phase
L	Liquid phase
l,b	Large bubbles
out	Outlet value
s,b	Small bubbles
trans	Transition

conversion due to kinetic limitations [5]. Thus, catalyst development has been a very active research area for improved methane conversion at reasonably low operating temperatures, enhanced H_2 yields, as well as controlled carbon properties (e.g., [6–8]). Separation of the produced carbon from conventional solid catalysts is a potentially showstopping challenge due to difficulties in collecting the valuable carbon products, rapid catalyst deactivation, and clogging of the reactor, requiring additional catalyst regeneration steps [9]. A recent study evaluated the use of an iron-based catalyst for methane pyrolysis in TGA followed by a techno-economic assessment. It has shown that hydrogen production cost could be competitive with SMR-CCS if 20% of produced carbon is recovered and sold at $1.1–1.35/kg [10]. Catalyst regeneration should however be considered through direct carbon combustion or gasification that are associated with extra CO_2 emissions. The study also investigated a scenario that could remove the need for catalyst regeneration, but this assumes high recovery of the produced carbon which is unlikely to be realistically feasible using the proposed fluidized bed concept. Additionally, logistics for catalyst supply and waste handling should be investigated, if such a process is to be successfully upscaled for industrial deployment.

These challenges have prompted a shift in research focus to liquid-based reactors such as molten metal [11]. In this concept, methane is passed through a molten metal bath (maintained at operating temperatures favouring pyrolysis) in which the solid carbon product can float by buoyancy to the melt surface, thus facilitating its recovery while the gaseous products leave for further processing. Several studies have been completed investigating the suitability of different metals for the process (Tin [11], Tellurium [12], Gallium [13], or mixtures such as Nickel & Bismuth [14]), where methane conversion up to 95% was reported [14]. Two key challenges were however reported: i) high conversion was only achieved at very low feed rates [11] (very high gas residence time) and ii) the carbon product contained metal impurities (83% carbon purity when a mixture of Ni and Bi was used [15]).

Molten salts offer another promising avenue to unlocking the potential of liquid-based methane pyrolysis. This approach can capitalize on the wide variety of existing commercial salts, thus offering multidimensional opportunities for enhancing the process performance. Screening studies focussed mainly on alkali-halide salts that are industrially attractive due to their low cost, high temperature stability, and non-toxicity [16] (i.e., NaCl, NaBr, KCl, and KBr). Activation energies close to 300 kJ/mol were measured for those salts in a bubble column [16], outperforming the homogeneous uncatalyzed reaction (420 kJ/mol). The activation energy can be further reduced to 167 kJ/mol when a mixture of KCl & $MnCl_2$ is used [17]. Similar values were reported when a 2.5 wt% Mn/Co solids catalyst was dispersed in a melt formed of a mixture of NaBr and KBr (175.5 kJ/mol) [18] and when a 3 wt% iron based catalyst was added in the form of $FeCl_3$ to a mixture of NaCl-KCl (171 kJ/mol) [19].

Graphitic carbon was reported in several of the tested salts, indicating the possibility of achieving high value carbon targeting the growing market of C anodes for battery and metal production industries. However, the carbon purity remains an issue even after carbon washing (96% was achieved for KCl/$MnCl_2$ mixtures [17]), but high temperature heat treatments were reported to be effective at cleaning the residual salt from the carbon, presumably due to selective evaporation of the salt [16].

Limited techno-economic assessment studies were completed on liquid-based methane pyrolysis reactors. At a carbon price exceeding $21 t^{-1} CO_2 equivalent, a molten Ni-Bi based pyrolysis process was considered to compete favourably to SMR with carbon capture and sequestration [20]. Another study investigated the cost performance of molten gallium-based methane pyrolysis identifying the scenarios in which this process can compete with SMR based hydrogen production [13].

The present study focuses on molten salt pyrolysis using a catalytically active KCl/$MnCl_2$ mixture reported to achieve a reasonably good catalytic performance [17]. A thorough techno-economic assessment will reveal the optimal reactor operating conditions, potential added costs related to salt handling, sensitivity to key market factors, and the prospects of more expensive first-of-a-kind plants. The primary objective of the study is to estimate the potential of turquoise hydrogen as a supply option in a future hydrogen economy.

2. Methodology

This section first describes the molten salt pyrolysis process evaluated in this study, followed by sections detailing the methods behind the process and reactor modelling, economic assessment, and performance quantification.

2.1. Process description

The molten salt pyrolysis process is depicted in Fig. 1 with stream data in Table 3. Natural gas enters from the grid (stream 1) and is preheated to 300 °C for desulphurization (stream 2) before being sent to the pyrolysis reactor (stream 3). This main reactor unit is electrically heated and operates at 1000 °C and an optimal pressure of 12 bar. The reactor outlet (stream 4) is split, with part of the stream being cooled down to provide a quench at the top of the reactor (stream 5) to limit the amount of salt exiting in vapour form. Pure carbon is also produced from

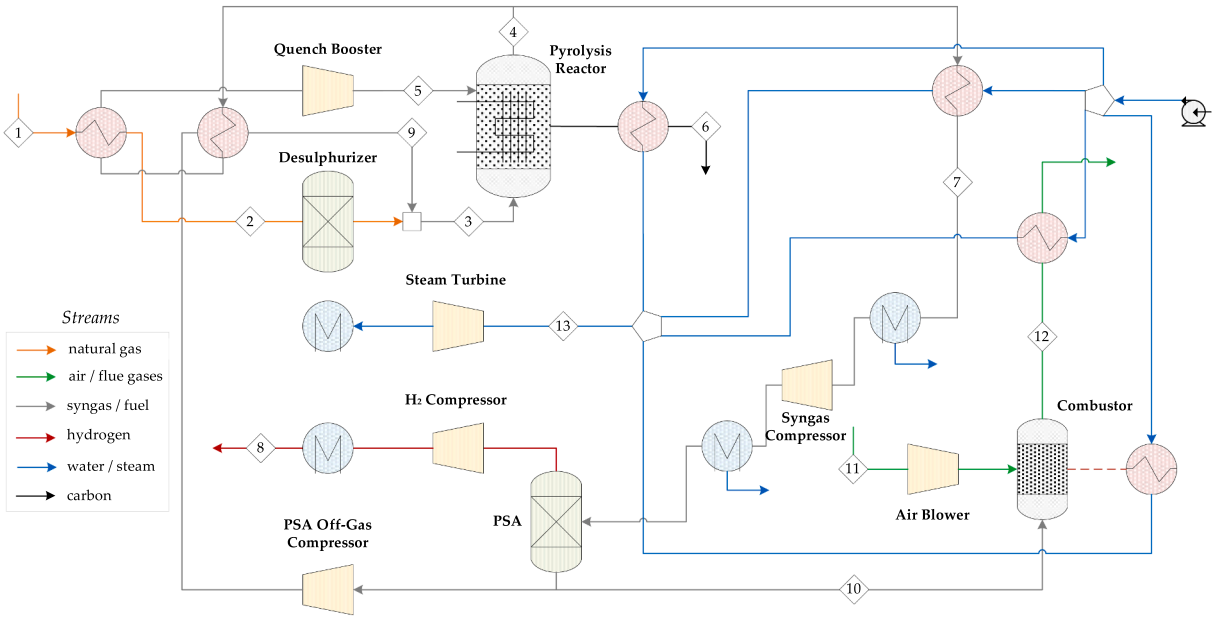

Fig. 1. Flowsheet of the process layout considered in this study.

the reactor (stream 6). The remaining H_2-rich reactor outlet gases are cooled and compressed (stream 7) before the PSA unit operating at 30 bar to separate out the pure hydrogen product at a 60-bar delivery pressure (stream 8). 95% of the PSA off-gas is recycled to the pyrolysis reactor (stream 9) to maximize H_2 and C production efficiency and minimize CO_2 emissions. However, a small fraction (5% in this case) must be combusted (stream 11 supplies the air for combusting the fuel in stream 10) to prevent excessive accumulation of N_2 in the system. Finally, steam is raised from various sources in the plant at 565 °C and 140 bar (stream 13), mimicking a commercially available industrial steam cycle[1], with heat rejection at 40 °C and around 0.08 bar. The main assumptions implemented in the process simulations are summarized in Table 1.

Table 1
Key assumptions implemented in the process simulations.

Parameters	Values	Units
H_2 production rate	0.75	Kg/s
Compressor isentropic efficiency	85	%
Compressor mechanical efficiency	90	%
Turbine isentropic efficiency	92	%
Turbine Mechanical efficiency	98	%
Temperature approach in the pyrolysis reactor	50–150	°C
Minimum approach in heat exchangers	10	°C
Pressure drop in heat exchangers (gas)	2	% of inlet stream
Pressure drop in heat exchangers (liquid)	0.4	bar
Water exit temperature from cooling tower	20	°C
H_2 delivery pressure	60	bar
H_2 temperature after compression	50	°C
Natural gas pre-heating temperature	300	°C
Natural gas inlet temperature	15	°C
Steam turbine inlet temperature	550	°C
Turbine outlet temperature	40	°C
Excess air flow rate in combustor	1.2 times	Stoichiometric requirement

[1] https://www.ge.com/steam-power/products/steam-turbines/stf-a100

2.2. Process model

The process model was developed in ASPEN PLUS V10 (Aspen technology, Inc) to perform the heat and mass balance calculations considering the thermodynamics equilibrium in all the components. The Peng-Robinson (PR) property method was used to evaluate the properties for the hydrocarbon streams while IAPWS-95 method was used to estimate the properties of steam. The pyrolysis reactor was modelled using the REQUIL reactor module based on a specified temperature approach, i.e., conversion is set to equilibrium at a specified temperature below the reactor operating temperature to represent incomplete conversion from reaction rate limitations. The combustor was modelled as RGIBBS module, predicting essentially complete conversion of the fuel. The PSA was modelled as a splitter and the H_2 recovery was estimated based on a literature correlation [21]. Carbon was defined as solid graphite.

2.3. Reactor model

The molten salt pyrolysis reactor is modelled as a bubble column reactor based on the methodology of Wilkinson, Spek [22] (Eq. (1) – Eq. 5), which allows the gas holdup (ϵ_G) and rise velocity of small ($U_{s,b}$) and large ($U_{l,b}$) bubbles to be estimated as a function of the liquid and gas properties, and the superficial gas velocity (U_G).

$$U_{s,b} = 2.23\frac{\sigma_L}{\mu_L}\left[\frac{{\sigma_L}^3\rho_L}{g\mu_L^4}\right]^{-0.273}\left[\frac{\rho_L}{\rho_G}\right]^{0.03} \quad (1)$$

$$U_{G,trans} = 0.5U_{s,b}\exp\left(-193\rho_G^{-0.61}\mu_L^{0.5}{\sigma_L}^{0.11}\right) \quad (2)$$

$$U_{l,b} = U_{s,b} + 2.4\frac{\sigma_L}{\mu_L}\left[\frac{\mu_L\left(U_G - U_{G,trans}\right)}{\sigma_L}\right]^{0.757}\left[\frac{{\sigma_L}^3\rho_L}{g\mu_L^4}\right]^{-0.077}\left[\frac{\rho_L}{\rho_G}\right]^{0.077} \quad (3)$$

$$For U_G \le U_{G,trans}, \epsilon_G = \frac{U_G}{U_{s,b}} \quad (4)$$

$$For U_G > U_{G,trans}, \epsilon_G = \frac{U_{G,trans}}{U_{s,b}} + \frac{U_G - U_{G,trans}}{U_{l,b}} \quad (5)$$

The Wilkinson method assumes that all gas is present as small bubbles rising with a velocity of $U_{s,b}$ in the homogenous bubbling regime

($U_G < U_{G,trans}$). Above the transition to the churn turbulent regime ($U_G > U_{G,trans}$), all additional gas volume occurs in the form of large bubbles rising with velocity $U_{l,b}$ (Eq. 5). Therefore, assuming that conversion of methane occurs in parallel in small and large bubbles as a first-order reaction, and integrating over the height of the reactor, the methane concentration at the reactor outlet can be estimated with Eq. (6).

$$C_{CH_4,out} = \frac{C_{CH_4,eq} + \epsilon_{s,b}\left(-\frac{k}{U_{s,b}}H + \ln\left(C_{CH_4,in} - C_{CH_4,eq}\right)\right) + \epsilon_{l,b}\left(-\frac{k}{U_{l,b}}H + \ln\left(C_{CH_4,in} - C_{CH_4,eq}\right)\right)}{\epsilon_{s,b} + \epsilon_{l,b}} \quad (6)$$

In this study, a molten salt mixture of 50 mol% $MnCl_2$ with KCl is considered, which shows some of the fastest kinetics for molten salt pyrolysis published in the open literature to date [23]. Adjusting the units in the aforementioned reference based on the reported bubble diameter of 6 mm, the reaction rate constant used in Eq. (6) becomes $k = k_0 \exp\left(-\frac{E_A}{RT}\right)$, with $k_0 = 4.3 \times 10^{51}\frac{1}{s}$ and $E_a = 153\frac{kJ}{mol}$. It is therefore assumed that a similarly small bubble size can be obtained in the industrial reactor as in the lab-scale experiments where the kinetics were obtained. This may be an optimistic assumption, which was countered by the conservative assumption of sizing the reactor based on the large gas volume observed at the top of the reactor after volume expansion from the conversion of one mole of CH_4 into two moles of H_2.

The temperature-dependent molten salt properties used in Eq. (1) – Eq. 5 are specified as follows. The density of $MnCl_2$ and KCl were obtained from Janz, Dampier [24] and the surface tension and viscosity of KCl from Janz [25]. The surface tension of $MnCl_2$ was estimated based on the theoretical model of Aqra [26], using the heat of sublimation determined by Murthy and Dadape [27]. The viscosity of $MnCl_2$ was estimated using the modified rough hard-sphere model of Wang and Teja [28]. The mixture density was approximated as an ideal mixture and the mixture surface tension was calculated as a simple molar average, considering the similar surface tensions of $MnCl_2$ and KCl. The mixture viscosity was estimated using the unit-cell model of Zhao, Hu [29].

To size the reactor for the economic assessment, it is assumed that the reactor is operated at a superficial gas velocity that yields a reactor aspect ratio close to 7, including a freeboard region in the top third of the reactor. This yields a liquid bath aspect ratio of a little under 5, which is typical for industrial bubble columns [30], and a gas void fraction in the 36–50% range. In the case with the lowest operating pressure, the superficial gas velocity was restricted to keep the void fraction below 50%, yielding a reactor aspect ratio around 6. No clear recommendation for the maximum achievable void fraction could be found in the literature, but this uncertain assumption does not have a large influence on the cost assessment. For example, in the central case with a 12-bar operating pressure, halving the superficial gas velocity reduced the aspect ratio from 6.9 to 3.2 and the void fraction from 44% to 34%, causing only a 1% increase in the total production cost of carbon and hydrogen.

The required reactor diameter is calculated based on the specified superficial gas velocity and the volumetric flow rate of gas at the top of the bath, whereas the bath height to achieve the outlet methane concentration resulting from each process simulation is calculated from Eq. (6). These calculations are done iteratively to reach a reactor aspect ratio around 7. As mentioned earlier, the reactor height includes a freeboard of 50% the bath height, giving sufficient space for the formation of the carbon layer on top of the bath and for applying a gas quench to cool the outlet gases to prevent large losses of evaporated salt.

2.4. Economic assessment

The pyrolysis plants in this study were economically evaluated using in a dedicated tool for standardized economic assessment of novel chemical and energy plants [31] (a detailed user's guide is available [32]). The tool facilitates bottom-up economic analyses using general cost correlations for standard equipment like heat exchangers, vessels, and turbomachinery from Turton et al. [33] or simplified scaling correlations for more complex units with costs available in the literature. For example, the present study scaled the cost of the PSA from Spallina et al. [34].

Two process vessels were assumed to represent the pressurized pyrolysis reactor: an inner reactor vessel made from expensive nickel alloy to carry the thermal and corrosive loads and a thick outer pressure shell constructed from carbon steel to carry the pressure load. A 20 cm insulation layer is assumed between these two vessels to ensure that the pressure shell remains at a low temperature to maintain its mechanical strength. Furthermore, the inner reactor vessel cost is increased by 50% to account for elements such as gas distributors and a mechanism for removing the solid carbon. Electrical heating elements are added using fully installed transformer and heating wire costs of 17.3 $/kW and 3.3 $/kW, respectively [35]. It is possible that the transformer can be avoided, but its cost was retained as a conservative assumption. Finally,

Table 2
Economic evaluation assumptions.

Capital estimation methodology		
Bare Erected Cost (BEC)		SEA Tool Estimate
Engineering Procurement and Construction (EPC)		10% of BEC
Process contingency (PS) – applied to the pyrolysis reactor		30% of BEC
Project Contingency (PC)		20% of (BEC + EPC + PS)
Total Plant Cost (TPC)		BEC + EPC + PS + PC
Owner's Costs (OC)		15% of TPC
Total Overnight Costs (TOC)		TPC + OC
Operating & maintenance costs		
Fixed		
Maintenance	2.5	%TOC
Insurance	1	%TOC
Labour	60	k€/y/person
Operators	20	Persons
Variable		
Natural gas	6.5	€/GJ
Electricity	60	€/MWh
Process water	6	€/ton
Make-up water	0.35	€/ton
CO_2 tax	100	€/ton
Salt make-up	2	€/kg
Salt lifetime	2	years
Hydrogen sales price *	1.6	€/kg
Cash flow analysis assumptions		
1st year capacity factor	65	%
Remaining years	85	%
Discount Rate	8	%
Construction period	3	years
Plant Lifetime	25	years

*Implemented as a negative cost.

Table 3
Stream data for the numbered streams in Fig. 1.

Stream	m (kg/s)	T (°C)	P (bar)	Mol fractions									
				CH_4	C_2+	H_2	CO	H_2O	CO_2	N_2	O_2	Ar	C
1	3.431	15.0	13.64	0.890	0.081				0.020	0.009			
2	3.431	300.0	13.37	0.890	0.081				0.020	0.009			
3	5.985	466.2	13.37	0.663	0.044	0.129	0.054	0.002	0.012	0.097			
4	5.132	745.7	12.00	0.121		0.767	0.036	0.013	0.001	0.062			
5	1.574	104.9	12.00	0.121		0.767	0.036	0.013	0.001	0.062			
6	2.428	93.0	12.00										1.000
7	3.558	95.0	11.76	0.121		0.767	0.036	0.013	0.001	0.062			
8	0.750	50.0	60.00			1.000							
9	2.554	726.0	13.37	0.392		0.282	0.118	0.004	0.002	0.201			
10	0.134	30.0	1.02	0.392		0.282	0.118	0.004	0.002	0.201			
11	1.387	15.0	1.00					0.010		0.774	0.207	0.009	
12	1.522	1150	1.00					0.173	0.079	0.710	0.030	0.008	
13	5.936	565.0	140.00					1.000					

an additional process contingency of 30% is applied to the pyrolysis reactor in acknowledgement of the high degree of uncertainty in the cost assessment of this novel unit.

The bare erected cost of all the equipment in the plant is automatically scaled for currency, year, and location. Subsequently, fixed and variable operating costs are added and the levelized cost of carbon is determined in a discounted cash flow analysis setting the net present value to zero (described in more detail in the "Performance Measures" section below). Table 2 outlines the main assumptions employed in the economic assessment and the complete economic assessment files for each case can be viewed online[2].

2.5. Performance metrics

Energy efficiency is quantified by defining efficiencies for hydrogen (Eq. (7)), carbon (Eq. (8)), and electricity (Eq. (9)) based on the mass flow rates ($\dot{m}$) and lower heating value (LHV) of output products and input fuel. It is noted that the electric efficiency (η_{El}) is negative in this study as all the plants consume considerable power for heating the pyrolysis reactor. In addition, an overall efficiency (Eq. (10)) is defined as the sum of these three efficiencies, implying that hydrogen, carbon, and electricity are weighed equally in terms of economic value.

$$\eta_{H_2} = \frac{\dot{m}_{H_2} LHV_{H_2}}{\dot{m}_{NG} LHV_{NG}} \tag{7}$$

$$\eta_{C} = \frac{\dot{m}_{C} LHV_{C}}{\dot{m}_{NG} LHV_{NG}} \tag{8}$$

$$\eta_{El} = \frac{\dot{W}_{net}}{\dot{m}_{NG} LHV_{NG}} \tag{9}$$

$$\eta = \eta_{H_2} + \eta_{El} + \eta_{C} \tag{10}$$

CO_2 avoidance is quantified as the fraction of carbon in the fuel that is transformed to a pure carbon product instead of being converted to CO_2 and emitted to the atmosphere. As shown below, the mass flow rate of the carbon product is converted to the flowrate of CO_2 that would be produced if it was combusted using molar weights (M_r) and then compared to the actual CO_2 emissions from the plant.

$$CA = \frac{\dot{m}_C \frac{M_{r,CO_2}}{M_{r,C}}}{\dot{m}_{CO_2,emit} + \dot{m}_C \frac{M_{r,CO_2}}{M_{r,C}}} \tag{11}$$

The primary economic indicator in the present study is the levelized cost of carbon ($LCOC$). It is quantified as the carbon sales price required to set the net present value (NPV) to zero at the end of the plant's economic lifetime (n), assuming a certain discount rate (i). In Eq. (13), the annual cash flow in year t (ACF_t) is defined as the sum of variable and fixed cash flows. Variable cash flows include revenues from carbon (R_C) and hydrogen (R_{H_2}) sales and variable operating costs (C_{VOM}), which is mainly electricity purchases. These cash flows are determined by finding the maximum possible revenues or cost per year and multiplying by the capacity factor (ϕ). Fixed cash flows involve capital expenditures during the construction period of the plant ($C_{capital}$) and fixed operating and maintenance costs (C_{FOM}). The NPV is then set to zero by adjusting the $LCOC$ in Eq. (14), where P_C is the maximum annual production of carbon achievable.

$$NPV = \sum_{t=0}^{n} \frac{ACF_t}{(1+i)^t} \tag{12}$$

$$ACF_t = \phi \cdot (R_C + R_{H_2} - C_{VOM}) - C_{capital} - C_{FOM} \tag{13}$$

$$R_C = LCOC \cdot P_C \tag{14}$$

3. Results and discussion

Results from the study are presented and discussed in five sections. The first two sections aim to form a clear understanding of the molten salt pyrolysis process by studying two key optimization variables: reactor pressure and equilibrium approach in the reactor. In the third section, the cost of stricter salt-handling measures is quantified. A sensitivity analysis to key market parameters is presented in the fourth section. Finally, the overall techno-economic potential of the process is put into context by exploring the market potential for high-purity carbon at different price points.

3.1. Effect of pressure

Reactor pressure is an important optimization variable in the molten salt pyrolysis process. Higher pressures reduce costly hydrogen compression work and intensifies the reactor, but equilibrium is negatively affected, leading to lower conversion. Incomplete fuel conversion can be counteracted by recycling most of the PSA off-gas back to the pyrolysis reactor. However, such recycling involves considerable costs in the form of a recycle compressor and higher gas throughput rate in all most process units, leading to higher capital and operating costs.

This trade-off is studied by operating the reactor at pressure levels of 5, 12, and 32 bar. The PSA is always operated at 30 bar, requiring additional syngas compressors prior to the PSA for the 5 bar (two compression stages) and 12 bar (one compression stage) cases. 95% of the PSA off-gas is recycled back to the electrically heated pyrolysis reactor operating at 1000 °C, with the remaining 5% being combusted to avoid excessive N_2 accumulation in the recycle loop. An equilibrium

[2] https://bit.ly/39BKDYJ

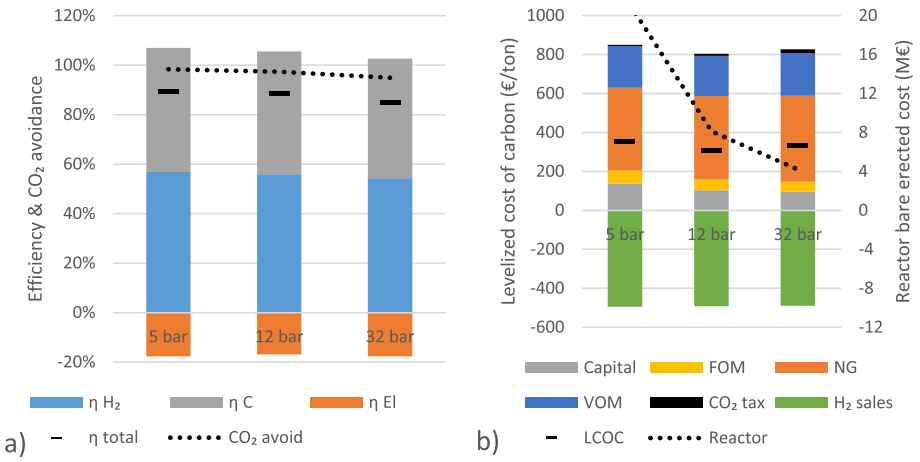

Fig. 2. The effect of reactor pressure on the technical (a) and economic (b) performance of the pyrolysis plant.

approach temperature of 150 °C is used in all cases to limit natural gas conversion and allow the reactor size to be estimated.

Figure 2a shows the technical performance of the plant as a function of the reactor pressure. An increase in reactor pressure causes a decrease in the output of hydrogen and carbon due to the lower conversion rates achieved in the reactor. However, electric power consumption also decreases with pressure as lower compression requirements before the PSA and higher steam turbine power output outweigh increased power consumption from the recycle compressor. Overall efficiency peaks in the 12-bar case at 88.7%. CO_2 emissions are minimized due to the 95% PSA off-gas recycle to ensure a high level of CO_2 avoidance. However, CO_2 avoidance falls with reactor pressure as lower conversion rates in the reactor create a larger PSA off-gas stream with a higher methane fraction, leading to greater CO_2 emissions when 5% of this stream is combusted.

Regarding economic performance, Fig. 2b shows that the 12-bar case also achieves the lowest LCOC at 312 €/ton. Even though the 5-bar case has a higher carbon efficiency, reducing natural gas costs, higher electricity and capital costs outweigh this benefit. The reactor cost increases especially strongly in the 5-bar case due to the higher volume of gas that must be processed. The higher degree of conversion also increases the required gas residence time, further increasing the reactor volume. When the reactor pressure is increased to 32 bar, the reactor cost reduces further, but the total capital costs remain similar to the 12-bar case. The large recycle stream in this case increases the size of several process units, cancelling out the benefits from further intensification of the reactor. A similar optimum of 10 bar was found for an iron based catalytic methane reforming process [10].

Based on these results, the 12-bar case is selected for further study.

3.2. *Effect of approach temperature*

Slow reactions are a key challenge in natural pyrolysis. Traditional catalysis cannot be used because carbon will quickly deposit on the catalyst surface, rendering it inactive. Molten salts with catalytic properties like the $MnCl_2$ considered in the present study can mitigate this challenge, but kinetic limitations remain a considerable challenge when the reactor is operated at a reasonable temperature. 1000 °C was selected in the present study as a good compromise between relatively fast kinetics on the one hand and feasible reactor construction with limited salt evaporation on the other.

Methane conversion is limited below equilibrium by imposing an equilibrium approach temperature in the reactor. For example, if the approach temperature is set to 100 °C, the reactor achieves equilibrium at 900 °C, even though the reactor temperature is set to 1000 °C. The simplified reactor model described in Eq. (1) – Eq. (6) is then used to estimate the reactor size required to reach the degree of methane conversion at the given approach temperature.

Figure 3a shows that varying the approach temperature within the range of 50–150 °C only had minor effects on the technical and economic performance of the plant. A mild gain in hydrogen and carbon efficiency is achieved by a narrower temperature approach as more conversion is achieved. However, this effect is moderated by the 95% recycle stream that recycles most of the unconverted methane back to

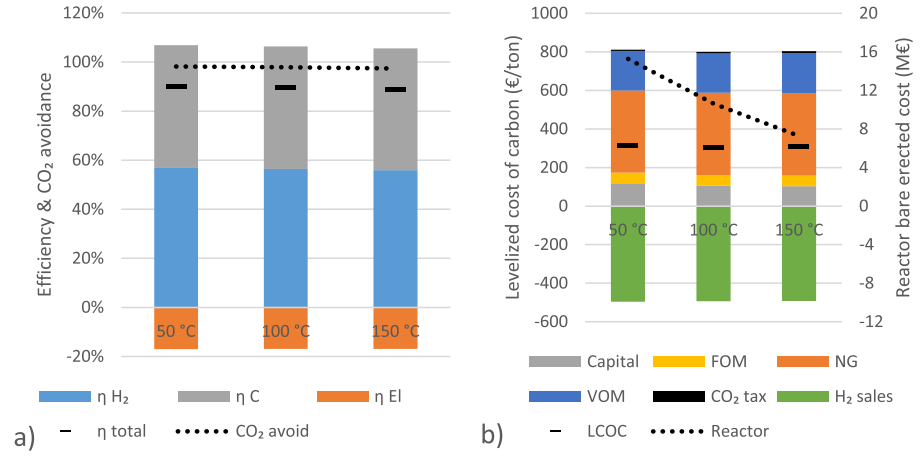

Fig. 3. The effect of equilibrium approach temperature on the technical (a) and economic (b) performance of the pyrolysis plant.

the reactor. A similarly mild trend is observed for CO_2 avoidance, where narrower temperature approaches slightly reduce CO_2 emissions due to a lower fraction of unconverted methane in the 5% of the PSA off-gas that is combusted. Overall, decreasing the approach temperature from 150 °C to 50 °C increased overall efficiency by 1.2 %-points and CO_2 avoidance by 0.7 %-points.

A similarly mild effect of the temperature approach on economic performance is observed in Fig. 3b. Overall, the 100 °C temperature approach slightly outperforms the other cases, reaching a LCOC of 306 €/ton. The 50 °C case has slightly lower natural gas and CO_2 taxation costs as well as slightly higher revenues from hydrogen sales, but the more expensive reactor required to achieve higher fuel conversion outweighs these benefits. The 150 °C case shows similar capital costs to the 100 °C case, as higher capital costs from greater recycling cancel out further reductions in the reactor cost. Thus, slightly higher fuel and CO_2 costs cause a mild increase in the LCOC.

Based on these results, the case with a 100 °C approach temperature will be used in the remainder of the study.

3.3. Potential additional costs for salt handling

There are two potential technical challenges related to the salt: 1) small fractions of evaporated salt exiting the reactor and fouling downstream heat exchangers and 2) small fractions of salt remaining in enclosed spaces within the carbon product even after washing. This section will investigate the additional costs that may be required to deal with these challenges.

Salt evaporation can be minimized by lowering the temperature, and therefore the vapour pressure, in the freeboard region above the molten salt bed. This can be done by quenching with cold gas above the molten salt bed, as deployed in the previous cases where the reactor outlet temperature is quenched to about 750 °C. However, more quenching may be needed to reduce salt evaporation to acceptable levels. For example, the $MnCl_2$ salt in the mixture modelled in this study has a vapor pressure of 0.0055 bar at the current reactor outlet. Applying Raoult's law to the 50/50 mixture of $MnCl_2$ and KCl indicates that there will be about 160 ppm of evaporated salt the outlet stream. Even though such a fraction sounds negligible, it will take only about four days for a 1 mm fouling layer to build up on the downstream heat exchangers if all the evaporated salt deposits on the surfaces. Thus, another case will be completed to study the effect of additional quenching to 510 °C where the salt concentration in the outlet gas reduces to 6 ppm. However, the larger recycle stream required to do this additional quenching means that the reactor outlet flowrate doubles. In this case, a 1 mm fouling layer will take about two months to form if all the entrained salt deposits in the downstream heat exchangers, which is a more reasonable timescale for periodic cleaning.

For removing all traces of salt from the carbon, an electrically heated shaft furnace will be employed where the carbon is heated to 1450 °C, which is above the boiling point of KCl at atmospheric pressure. In practice, a microwave system may be required to ensure uniform heating of the product to such high temperatures. Although resistance heating elements above this temperature are available (e.g., molybdenum disilicide elements with the potential to reach 1800 °C), more costly microwave heating at 400 $/kW (a rough estimate from Alibaba.com) is used in the cost assessment as a conservative assumption. In addition, a small recycled N_2 purge gas will be required to transport any evaporated salt out of the furnace and ensure that the carbon is loaded and removed in an inert atmosphere to avoid any oxygen from entering and combusting the valuable pure carbon product. In the process flowsheet, however, this added unit it is modelled simply as an electrical heater from 100 °C (the carbon washing temperature) to 1450 °C, followed by a steam generating heat exchanger cooling the carbon product back down to 60 °C. Steam from the carbon cooling is fed to the steam turbine to recover some of the electricity used to heat the carbon. This additional process component will be added to the case with the quench to 500 °C described above.

Results are illustrated in Fig. 4. Hydrogen and carbon efficiencies and CO_2 avoidance remain unchanged by these two salt treatment methods, but Fig. 4a shows that electric efficiency declines, especially with the thermal carbon cleaning. The large quench slightly reduces the efficiency of the power cycle because the reactor outlet temperature is reduced from 750 to 510 °C, making it impossible to reach the previous steam temperature of 565 °C. A heat integration scheme that utilizes the high-grade heat from PSA off-gas combustion to superheat steam raised from the reactor outlet gases could reach a maximum steam temperature of 500 °C. Due to this reduced temperature, the steam pressure was reduced from 140 bar to 100 bar to maintain similar turbine outlet conditions. This mild reduction in steam temperature only reduced the electric efficiency of the plant by 1.0 %-point. The electrically heated carbon purification had a larger effect on the electric efficiency of the plant, causing a 3.5 %-points reduction. Heating the carbon to 1450 °C consumes 9.0 MW of additional electricity, whereas the steam turbine output only increases by 3.5 MW due to the extra steam raised from cooling the carbon. When both measures are implemented simultaneously, the electric efficiency of the plant declines by 4.6 %-points.

Mirroring the technical results, the economic metrics in Fig. 4b show only a slight effect of the additional quench but a larger cost increase from the carbon heat treatment. The cost increases originate mostly from the additional electricity consumption, but some mild capital cost increases are also incurred. For the extra quench, these costs stem from a larger heat exchange network and a much larger quench recycle blower.

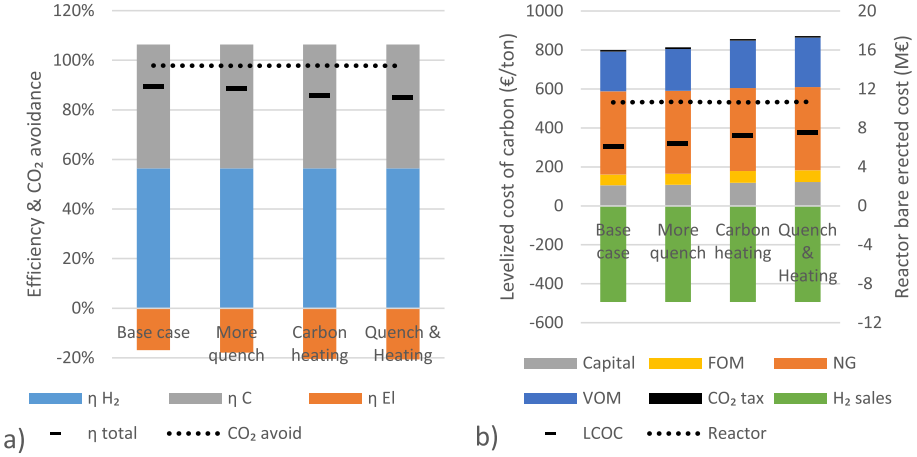

Fig. 4. The effect of additional quenching, heat treatment, and both measures combined on the technical (a) and economic (b) performance of the plant.

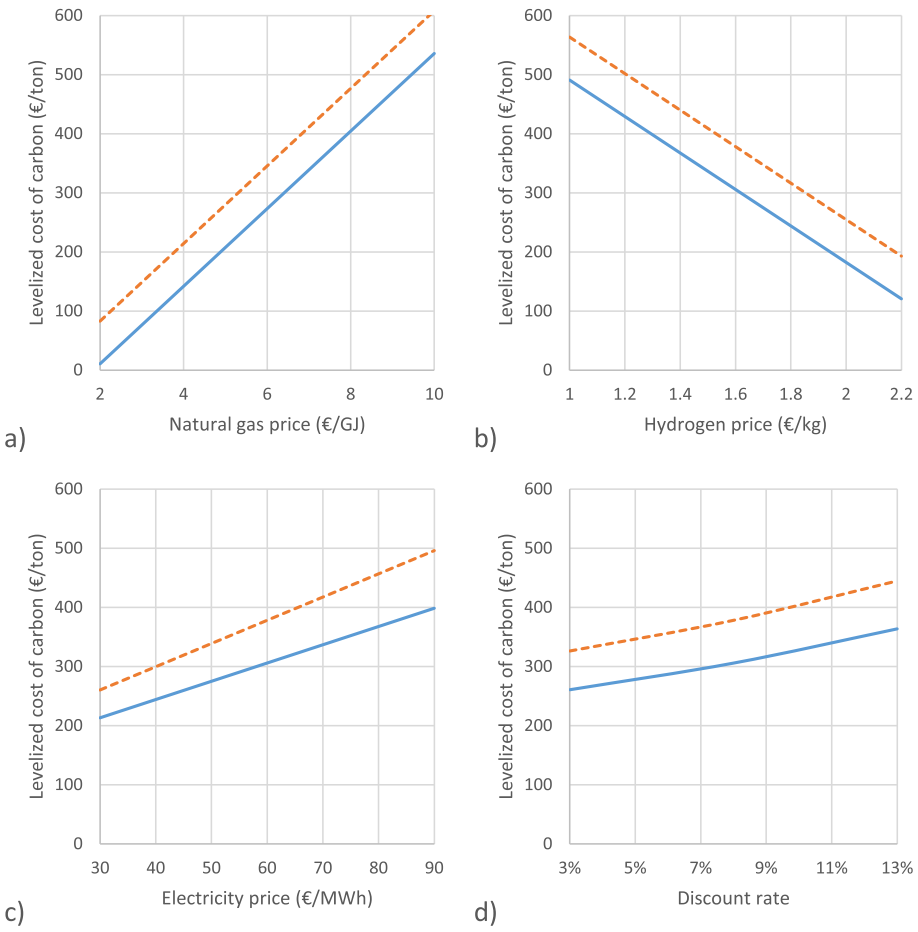

Fig. 5. Sensitivity of the levelized cost of carbon to four influential variables for the cases with (dashed line) and without (solid line) the additional salt-handling measures investigated in Fig. 4.

The cost of the electrically heated vessel causes the capital cost increase for the case with carbon heat treatment.

The mild effect of a larger quench is a positive sign, indicating that the potentially severe technical challenge of salt pollution of downstream equipment can be cheaply avoided. Thermal treatment of carbon will only be done if the end-use application demands essentially 100% pure carbon, which is likely to achieve a high selling price, justifying the somewhat larger cost escalation caused by this method. Overall, simultaneous implementation of these two measures increases the LCOC by 24%.

3.4. Sensitivity analysis

Several important market uncertainties exist in the present assessment. The effects of the four most influential ones are explored in Fig. 5. As shown in panel a, the natural gas price causes a LCOC range spanning more than 500 €/ton due to the wide uncertainty range of this parameter. Natural gas prices vary widely across the world and can also vary greatly in time due supply/demand imbalances. The default value of 6.5 €/GJ is representative of Europe in the International Energy Agency's Stated Policies Scenario [36], which is misaligned with the Paris climate agreement. The Paris-compatible Sustainable Development Scenario sees natural gas prices fall by about 30% by 2025 [36], staying constant thereafter as demand for fossil fuels declines. Producers like the USA and the Middle East enjoy consistently lower prices than Europe, whereas most large Asian economies pay higher prices due to an increasing reliance on liquified natural gas imports. It is interesting to observe that the LCOC almost goes negative when natural gas is very cheap at 2 €/GJ, which is achievable in gas-producing regions. Under such conditions, the revenues from hydrogen sales at the default value of 1.6 €/kg are sufficient to cover the expenses of the plant.

Since more than half of the energy output from the plant is hydrogen, Fig. 5b shows a large dependency on the hydrogen sales price. Higher hydrogen prices allow carbon to be sold at lower prices when expenses are kept constant. Future hydrogen prices are also uncertain, depending both on technological development and the cost of local input energy (natural gas for blue hydrogen and renewable electricity for green hydrogen). For perspective, a parallel study using an identical methodology and economic assumptions [37] showed that conventional steam methane reforming plants with pre-combustion CO_2 capture achieve hydrogen production costs around 2 €/kg, with more efficient process integrations potentially reaching 1.8 €/kg. Both these values are higher than the default value of 1.6 €/kg assumed in the present study, indicating significant upside potential.

It is also interesting to consider the required hydrogen sales price when no revenues are derived from carbon for comparison to 2.92–3.15 $/kg from a solid-catalysed pyrolysis process [10] (2.43–2.63 €/kg at a 1.2 $/€ conversion rate). Using a consistent natural gas price of 7 $/MMBTU, hydrogen costs from the present study are almost identical at 2.38–2.62 €/kg when the carbon sales price is zero.

Given the large consumption of electricity for heating the pyrolysis reactor, the electricity price also has a significant effect on the LCOC, as shown in Fig. 5c. Clean electricity costs from wind and solar are expected to continue declining in coming decades, but costs and complexities related to integrating ever-larger fractions of these variable and non-dispatchable electricity generators will dampen these cost declines. Furthermore, the quality of wind and solar resources varies widely across the world. The default cost of 60 €/MWh may be somewhat

optimistic for Europe, but regions with excellent solar and/or wind resources and ample space for deployment without facing public resistance may achieve considerably lower costs. Regions capable of constructing nuclear power at reasonable costs like China, Korea, and Russia [38] can also expect lower long-term electricity prices.

Finally, Fig. 5d shows a moderate effect of the discount rate, given that the plants evaluated in this study are not very capital intensive. The weighted average cost of capital (representative of the discount rate in practice) is generally higher in developing countries, and can fall to very low levels in developed countries when supporting policies guarantee investor returns, e.g., via guaranteed sales prices for wind and solar power regardless of their declining value as more capacity is installed. It is unlikely that fossil fuel technologies will ever benefit from such supportive policies, implying that investors will always be exposed to fluctuating fuel and product prices. Thus, the default discount rate of 8% should be reasonable for Europe and other developed economies.

3.5. Market potential

The potential of the molten salt pyrolysis process is closely linked to the size of the market for the high-purity carbon product. A rough estimation of carbon market size at three different price points is shown in Fig. 6. The first two price ranges are derived from current thermal and coking coal demand, whereas the third price is derived from the market for carbon anodes in the aluminium industry. In energy, metallurgical, and chemical applications, pure carbon should command a substantial price premium over coal because it contains about 30% more energy per ton, and it will not produce any ash or other harmful emissions (e.g., SOx). In Fig. 6, it is assumed that pure carbon can sell for about double the price per ton than coal alternatives due to these benefits. The lower bound of the third price range is derived from aluminium anodes available for about €500/ton on Alibaba.com. These anodes still contain about 2% sulphur, so the use of pure carbon to remove this emission source can command a substantial price premium. Other smaller markets like graphite or sorbents could pay substantially higher prices for high-purity carbon feedstock.

If hydrogen is to become the primary alternative to fossil fuels in the industrial, transportation, and heating sectors in the future, a need to sell carbon at high prices will restrict the molten salt pyrolysis process to the order of 1% of the potential hydrogen market. However, if carbon can be produced cheaply enough to compete in the metallurgical and chemical markets, the potential market size increases by a factor of about 20. Another halving in carbon production costs can access the even larger electricity & heat market. Although reaching this market will be difficult, it should not be neglected given that advanced processes with inherent CO_2 capture like the Allam power cycle [39] and chemical looping-based integrated gasification combined cycles [40] will benefit from using a pure carbon fuel. Thus, a good strategy will be to access high-value carbon markets to justify investments in more expensive first-of-a-kind plants, and enter lower-value-higher-volume markets when the technology is mature and costs have been successfully minimized.

The plant simulated in the present study produces about 65 kton of carbon per year. Thus, the high-price market range of 20–50 Mton of carbon can accommodate a sufficient number of plants to drive the cost down through experience and scale. As shown in Fig. 7, costs remain in the lower price range of the high-value carbon indicated in Fig. 6, even under pessimistic assumptions about reactor and overall plant costs. Initial plants may be able to access carbon prices towards the upper end of the indicated range by producing near-100% pure carbon via washing and heat treatment. Furthermore, clean hydrogen prices may be considerably higher than the 1.6 €/kg assumed by the time these early plants are built. As discussed around Fig. 5, if hydrogen costs are set by conventional blue hydrogen production plants, the LCOC could fall by around 100 €/ton.

For the long term, Fig. 3 shows that technologically mature molten salt pyrolysis plants could produce carbon at a cost that allows access to the much larger metallurgical and chemical markets. Such a large accessible carbon market makes the molten salt pyrolysis concept an attractive option for large-scale clean hydrogen production from natural gas in regions with strong opposition to CCS. Produced carbon can be used by local industry or exported for use in regions with access to cheap and publicly accepted CO_2 transport and storage facilities.

Further cost reduction potential exists if more catalytically active salts (or salt mixtures) can be discovered, with additional favourable properties like low vapour pressures, high density, and low wettability

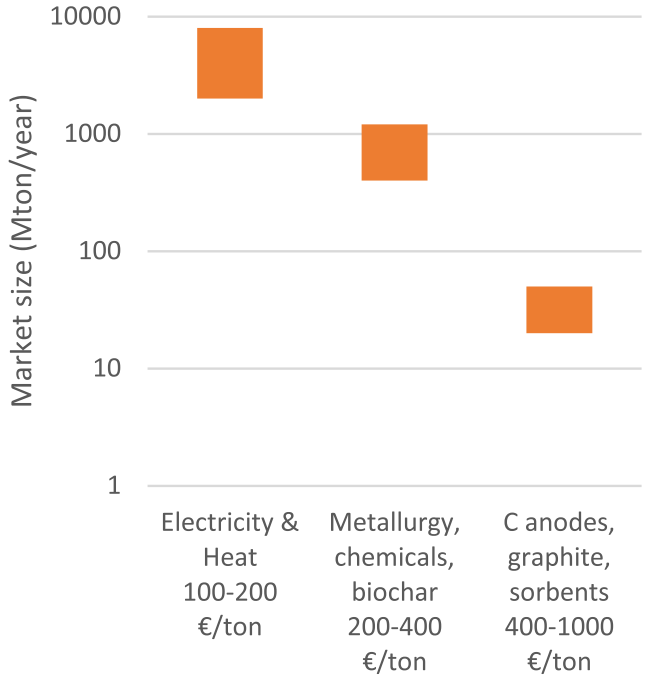

Fig. 6. Approximate carbon market size at three different price points.

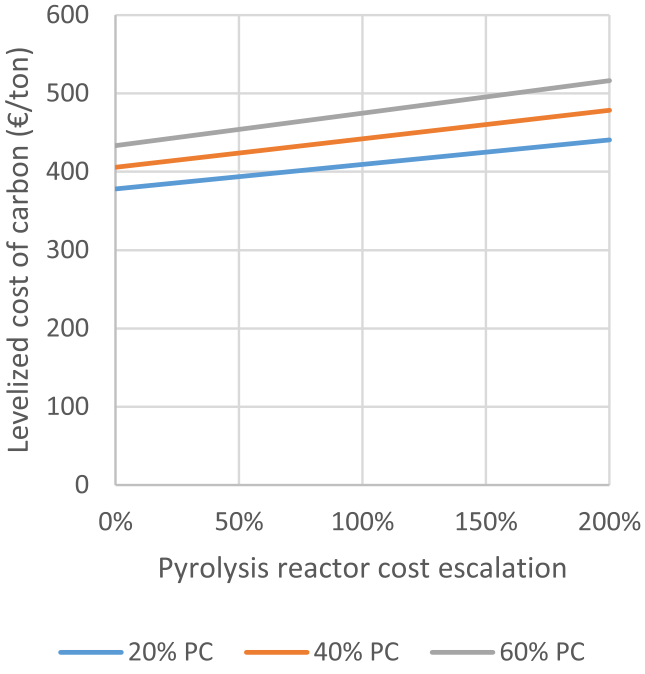

Fig. 7. Effect of higher reactor costs and project contingencies (PC) on the LCOC for the case with a quench temperature of 510 °C and additional heat treatment for carbon purification.

of carbon with the molten salt [41]. Such salts can allow for smaller reactors achieving greater conversion than the assumptions in the present study, while reducing costs related to salt cleaning and reactor outlet quenching. If reactor temperatures can be reduced, it could also enable a reactor design that facilitates heating via PSA off-gas combustion, much like conventional blue hydrogen production. Such a design will require a complex heat exchanger with internal combustion integrated into the reactor, but it can avoid the high consumption of expensive electrical energy for reactor heating. It will also require more of the PSA off-gas to be combusted, leading to higher CO_2 emissions.

4. Summary and conclusions

Molten salt pyrolysis is a promising new method for clean hydrogen production. Also known as turquoise hydrogen, pyrolysis can avoid much of the complexities facing conventional blue hydrogen production from steam methane reforming with CCS. The process is considerably more efficient because no steam is required, no exothermic water–gas shift reactions take place, and CO_2 capture and compression duties are avoided. These characteristics also help to reduce the process cost and inherently avoid any public resistance challenges facing CO_2 transport and storage infrastructure. However, the main economic challenge for deploying natural gas pyrolysis at scale is the size of the market for the pure carbon product.

The present study conducted a thorough techno-economic assessment of molten salt pyrolysis to assess its medium- and long-term potential. First, the effect of reactor operating pressure was investigated, finding that a pressure of 12 bar is optimal when operating the reactor at 1000 °C. Higher pressures can reduce reactor and H_2 compression costs, but low conversion due to equilibrium constraints makes PSA off-gas recycling increasingly expensive. This is exacerbated by the relatively slow reaction rates observed at 1000 °C, even for the catalytically active $KCl/MnCl_2$ salt mixture employed. Results showed that incomplete fuel conversion equivalent to equilibrium 100 °C below the reactor temperature gave the best compromise between reactor costs and process efficiency.

Two key technical challenges related to the salt were also investigated: salt vapour exiting the reactor to foul downstream heat exchangers and complete removal of salt from the carbon by heating the carbon product above the salt evaporation temperature. Additional quenching in the freeboard of the reactor to reduce the outlet temperature so that the evaporated salt fraction falls to only 6 ppm was attractively cheap, increasing the levelized cost of carbon by only 4.5%. The cost increase related to electrical heating to 1450 °C for carbon purification was larger at 18.6%. However, neither cost is prohibitive, indicating that these salt-related challenges are not showstoppers.

The levelized cost of carbon is highly sensitive to prices of natural gas, hydrogen, and electricity, and mildly sensitive to the discount rate. In the most suitable regions, molten salt pyrolysis could produce carbon for attractively low costs around 200 €/ton. Such a low cost grants access to large markets in metallurgical and chemical process industry and even energy applications. High-purity carbon from pyrolysis will command a substantial price premium over coal in these markets due to its higher energy density and avoidance of ash and other harmful emissions. If these large markets can be accessed, turquoise hydrogen can play a major role in the clean energy transition.

For the near-term, smaller but higher value carbon markets such as carbon anodes and graphite can facilitate the profitable construction of more expensive first-of-a-kind plants. Since the capital cost of the plant is relatively low, even a tripling of the reactor cost and the overall project contingency only caused moderate increases in the levelized cost of carbon. Under the most pessimistic assumptions, carbon needs to be sold around 500 €/ton, which should be accessible if the carbon is highly pure. Furthermore, carbon costs will fall to around 400 €/ton if hydrogen prices are set by conventional blue hydrogen production pathways. These economically viable early plants can then serve to reduce costs via learning and scale to access the much larger process and energy markets in the longer term.

Overall, the present study finds great promise in the molten salt pyrolysis process. Further research into demonstration and scale-up of this technology is strongly recommended.

CRediT authorship contribution statement

Florian Pruvost: Investigation, Methodology, Visualization, Writing – original draft. **Schalk Cloete:** Conceptualization, Methodology, Formal analysis, Investigation, Visualization, Supervision, Writing – original draft. **Jan Hendrik Cloete:** Investigation, Writing – original draft. **Chaitanya Dhoke:** Supervision, Writing – original draft. **Abdelghafour Zaabout:** Funding acquisition, Project administration, Conceptualization, Writing – original draft.

Declaration of Competing Interest

The authors declare that they have no known competing financial interests or personal relationships that could have appeared to influence the work reported in this paper.

Acknowledgement

The authors gratefully acknowledge the financial support of the Research Council of Norway under the FRINATEK program (project number: 302819).

References

[1] IEA, The future of hydrogen: Seizing today's opportunities. 2019, International Energy Agency.
[2] Keipi T, Tolvanen H, Konttinen J. Economic analysis of hydrogen production by methane thermal decomposition: comparison to competing technologies. Energy Convers Manage 2018;159:264–73.
[3] Abbas HF, Wan Daud WMA. Hydrogen production by methane decomposition: a review. Int J Hydrogen Energy 2010;35(3):1160–90.
[4] Keipi T, Tolvanen KES, Tolvanen H, Konttinen J. Thermo-catalytic decomposition of methane: the effect of reaction parameters on process design and the utilization possibilities of the produced carbon. Energy Convers Manage 2016;126:923–34.
[5] Weger L, Abánades A, Butler T. Methane cracking as a bridge technology to the hydrogen economy. Int J Hydrogen Energy 2017;42(1):720–31.
[6] Gutta N, Velisoju VK, Tardio J, Patel J, Satyanarayana L, Sarma AVS, et al. CH4 cracking over the Cu-Ni/Al-MCM-41 catalyst for the simultaneous production of H-2 and highly ordered graphitic carbon nanofibers. Energy Fuels 2019;33(12):12656–65.
[7] Hasnan NSN, Timmiati SN, Lim KL, Yaakob Z, Kamaruddin NHN, Teh LP. Recent developments in methane decomposition over heterogeneous catalysts: an overview. Mater Renew Sustain Energy 2020;9(2). https://doi.org/10.1007/s40243-020-00167-5.
[8] Musamali R, Isa YM. A novel catalyst system for methane decomposition. Int J Energy Res 2018;42(14):4372–82.
[9] Parmar KR, Pant KK, Roy S. Blue hydrogen and carbon nanotube production via direct catalytic decomposition of methane in fluidized bed reactor: capture and extraction of carbon in the form of CNTs. Energy Convers Manage 2021;232:113893. https://doi.org/10.1016/j.enconman.2021.113893.
[10] Riley J, Atallah C, Siriwardane R, Stevens R. Technoeconomic analysis for hydrogen and carbon Co-Production via catalytic pyrolysis of methane. Int J Hydrogen Energy 2021;46(39):20338–58.
[11] Plevan M, Geißler T, Abánades A, Mehravaran K, Rathnam RK, Rubbia C, et al. Thermal cracking of methane in a liquid metal bubble column reactor: experiments and kinetic analysis. Int J Hydrogen Energy 2015;40(25):8020–33.
[12] Zeng J, Tarazkar M, Pennebaker T, Gordon MJ, Metiu H, McFarland EW. Catalytic methane pyrolysis with liquid and vapor phase tellurium. ACS Catal 2020;10(15):8223–30.
[13] Perez BJL, et al. Methane pyrolysis in a molten gallium bubble column reactor for sustainable hydrogen production: proof of concept & techno-economic assessment. Int J Hydrogen Energy 2021;46(7):4917–35.
[14] Upham DC, Agarwal V, Khechfe A, Snodgrass ZR, Gordon MJ, Metiu H, et al. Catalytic molten metals for the direct conversion of methane to hydrogen and separable carbon. Science 2017;358(6365):917–21.
[15] Rahimi N, Kang D, Gelinas J, Menon A, Gordon MJ, Metiu H, et al. Solid carbon production and recovery from high temperature methane pyrolysis in bubble columns containing molten metals and molten salts. Carbon 2019;151:181–91.
[16] Palmer C, et al., Methane pyrolysis in low-cost, alkali-halide molten salts at high temperatures. Sustain Energy Fuels.

[17] Kang D, Rahimi N, Gordon MJ, Metiu H, McFarland EW. Catalytic methane pyrolysis in molten MnCl2 -KCl. Appl Catal B-Environ 2019;254:659–66.
[18] Patzschke CF, Parkinson B, Willis JJ, Nandi P, Love AM, Raman S, et al. Co-Mn catalysts for H-2 production via methane pyrolysis in molten salts. Chem Eng J 2021;414:128730. https://doi.org/10.1016/j.cej.2021.128730.
[19] Kang D, Palmer C, Mannini D, Rahimi N, Gordon MJ, Metiu H, et al. Catalytic methane pyrolysis in molten alkali chloride salts containing iron. ACS Catal 2020; 10(13):7032–42.
[20] Parkinson B, Tabatabaei M, Upham DC, Ballinger B, Greig C, Smart S, et al. Hydrogen production using methane: techno-economics of decarbonizing fuels and chemicals. Int J Hydrogen Energy 2018;43(5):2540–55.
[21] Nazir SM, Cloete JH, Cloete S, Amini S. Efficient hydrogen production with CO2 capture using gas switching reforming. Energy 2019;185:372–85.
[22] Wilkinson PM, Spek AP, van Dierendonck LL. Design parameters estimation for scale-up of high-pressure bubble columns. AIChE J 1992;38(4):544–54.
[23] Kang D, Rahimi N, Gordon MJ, Metiu H, McFarland EW. Catalytic methane pyrolysis in molten MnCl2-KCl. Appl Catal B 2019;254:659–66.
[24] Janz GJ, et al., Molten salts: volume 1. electrical conductance, density, and viscosity data, in NBS National Standard Reference Data Series (NSRDS). 1968.
[25] Janz GJ. Molten salts handbook. New York: Academic Press Inc.; 1967.
[26] Aqra F. Surface tension of molten metal halide salts. J Mol Liq 2014;200:120–1.
[27] Murthy BRK, Dadape VV. Vapour pressures of manganese chloride & study of the equilibrium reaction Mn(c)+MnCl2(g) = 2MnCl(g) at high temperatures. Indian J Chem 1968;6(12):714–7.
[28] Wang X, Teja AS. A modified rough hard-sphere model for the viscosity of molten salts. Fluid Phase Equilib 2016;425:47–50.
[29] Zhao Q-G, Hu C-X, Liu S-J, Chen X. A unit-cell model for predicting the viscosity of binary molten salts. Int J Heat Mass Transf 2017;107:484–8.
[30] Kantarci N, Borak F, Ulgen KO. Bubble column reactors. Process Biochem 2005;40 (7):2263–83.
[31] Arnaiz del Pozo C, Cloete S, Jiménez Álvaro Á. Standard Economic Assessment (SEA) Tool. Available from: https://bit.ly/3hyF1TT. 2021.
[32] Arnaiz del Pozo C, Cloete S, Jiménez Álvaro Á, SEA Tool User Guide. Available from: https://bit.ly/3jq9Bkf. 2021.
[33] Turton R, et al., Analysis, synthesis and design of chemical processes: Appendix A. 2008: Pearson Education.
[34] Spallina V, Pandolfo D, Battistella A, Romano MC, Van Sint Annaland M, Gallucci F. Techno-economic assessment of membrane assisted fluidized bed reactors for pure H2 production with CO2 capture. Energy Convers Manage 2016; 120:257–73.
[35] Stack DC, Curtis D, Forsberg C. Performance of firebrick resistance-heated energy storage for industrial heat applications and round-trip electricity storage. Appl Energy 2019;242:782–96.
[36] IEA, World Energy Outlook. 2020, International Energy Agency.
[37] Pruvost F, et al., Maximizing the techno-economic performance of steam methane reforming for near-term blue hydrogen production. Int J Hydrogen Energy, 2021. **Under review - Preprint and data:** https://bit.ly/3lViy4r.
[38] IEA, Projected Costs of Generating Electricity. 2020, International Energy Agency and Nuclear Energy Agency.
[39] Rodríguez Hervás G, Petrakopoulou F. Exergoeconomic analysis of the allam cycle. Energy Fuels 2019;33(8):7561–8.
[40] Arnaiz del Pozo C, et al. Integration of gas switching combustion and membrane reactors for exceeding 50% efficiency in flexible IGCC plants with near-zero CO2 emissions. Energy Convers Manage: X 2020;7:100050.
[41] Parkinson B, Patzschke CF, Nikolis D, Raman S, Dankworth DC, Hellgardt K. Methane pyrolysis in monovalent alkali halide salts: kinetics and pyrolytic carbon properties. Int J Hydrogen Energy 2021;46(9):6225–38.